*Int. J. Multiphase Flow* Vol. 13, No. 3, pp. 295–308, 1987
Printed in Great Britain. 

0301-9322/87 $3.00 + 0.00


# CALCULATION OF THE THERMODYNAMIC SOUND VELOCITY IN TWO-PHASE MULTICOMPONENT FLUIDS

D. J. PICARD† and P. R. BISHNOI‡

Department of Chemical and Petroleum Engineering, University of Calgary, Calgary, Alberta T2N 1N4, Canada

(*Received* 2 *August* 1985; *in revised form* 10 *October* 1986)

**Abstract**—The Peng–Robinson and Soave–Redlich–Kwong equations of state have been used to calculate the thermodynamic speed of sound in single-phase fluids consisting of pure components and mixtures, and in the two-phase region of a multicomponent mixture. The calculated velocities for single-phase fluids were compared with available data for methane, ethane, propane and a binary mixture of benzene in hexane. The basic trends observed in the data were predicted and in general, the comparison between theory and data was good.

Values calculated for the multicomponent mixture along an isobar showed a sudden drop in the thermodynamic sound velocity when the dew point temperature was reached. Inside the two-phase region the velocity decreased along an isobar with a lowering of temperature and increased suddenly when the other dew point or bubble point temperature was reached. At temperatures below the bubble or second dew point, the fluid behaved as a liquid, i.e. sound velocity increased with temperature. Similar overall behavior was predicted when the assumption of "frozen" sound velocity was employed except that a sudden drop did not occur at the dew point temperature of the mixture.

## 1. INTRODUCTION

For certain pure components, empirical correlations are available which enable the thermodynamic speed of sound, $a$, to be evaluataed in regions of non-ideal fluid behavior. Although these correlations are, at present, much more accurate than is possible through use of equations of state, they are available for only a few components and then are applicable over only limited ranges of temperature and pressure. In the absence of such correlations or experimental data, or for consideration of multicomponent mixtures, equations of state must, of necessity, be used.

In simulating the decompression characteristics of high-pressure natural gas in pipelines, Groves *et al.* (1978) presented a novel procedure for calculating the thermodynamic speed of sound in two-phase multicomponent fluids. By employing an ideal gas correlation for specific entropy, $s^\circ$ (superscript $^\circ$ denotes ideal gas property), and a thermal equation of state for prediction of phase behavior and departures from ideality, they were able to numerically solve for the thermodynamic speed of sound, given by

$$a^2 = \left(\frac{\partial P}{\partial \rho}\right)_s \qquad [1]$$

where $P$ is the absolute pressure and $\rho$ and $s$ are the mass density and specific entropy of the bulk fluid, respectively. To gain some insight into the nature of sound velocity inside the two-phase region of multicomponent fluids, this method is used to calculate $a$ along various isobars for the Prudhoe Bay gas described by Groves *et al.* For comparative purposes, these calculations are also performed using the frozen sound velocity approximation.

Since the selection of a suitable equation of state is important to both sets of calculations, an evaluation is made of two of the more popular equations used in the hydrocarbon processing industry, namely the Peng–Robinson (PR) equation of state (Peng & Robinson 1976) and the Soave–Redlich–Kwong (SRK) equation of state (Soave 1972). These equations are presented in appendix A. To evaluate the equations, calculated values of sound velocity are compared with available data for single-phase methane, ethane, propane and a binary mixture of benzene in hexane. Suitable data for two-phase multicomponent systems were not available.

†Present address: Western Research, Calgary, Alberta, Canada.
‡To whom correspondence should be addressed.

## 2. BACKGROUND

To determine the thermodynamic speed of sound in single-phase fluids, [1] is generally expressed in the more convenient form

$$a^2 = \frac{\gamma}{\rho\kappa}, \qquad [2]$$

where $\gamma$ is the specific heat ratio and $\kappa$ is the isothermal coefficient of volumetric expansion, which may be expressed as

$$\kappa = \frac{-1}{v}\left(\frac{\partial v}{\partial P}\right)_T. \qquad [3]$$

In [3], $T$ is the temperature of the fluid and $v$ is the specific volume.

For ideal gases, [2] reduces to the well-known form

$$a^{\circ 2} = \frac{\gamma RT}{M}, \qquad [4]$$

where $R$ is the universal gas constant and $M$ is the molecular weight.

With two-phase mixtures, a different computational approach must be taken since $\gamma$ and $\kappa$ are no longer clearly defined. For this purpose, Michaelides & Zissis (1983) presented two forms of [1] which are well-suited to the calculation of $a$ in pure two-phase fluids, namely

$$a^2 = \frac{v^2\left(\frac{dP}{dT}\right)^2}{\frac{c_{p_L}}{T} + \chi v_{LG}\frac{d^2P}{dT^2} - \frac{dP}{dT}\frac{dv_L}{dT}} \qquad [5]$$

or

$$a^2 = \frac{\left(\frac{v}{T}\right)^2\left(\frac{h_{LG}}{v_{LG}}\right)^2}{\frac{c_{p_L}}{T} + \chi v_{LG}\frac{d\left(\frac{h_{LG}}{Tv_{LG}}\right)}{dT} - \frac{h_{LG}}{Tv_{LG}}\frac{dv_L}{dT}}, \qquad [6]$$

where subscripts L and G denote the liquid and vapor phases respectively, subscript LG denotes latent quantity, $\chi$ is the fluid quality (i.e. mass of vapor per unit mass of the bulk fluid), $h$ is specific enthalpy and $v$ is a specific volume. In applying [5] and [6], $v$ is evaluated from the expression

$$v = (1-\chi)v_L + \chi v_G. \qquad [7]$$

If an accurate expression for saturation pressure were available, it was suggested that [5] could be used, otherwise correlations for $h_{LG}$, $v_{LG}$, $c_{p_L}$ and $v_L$ could be obtained and [6] used. Although appropriate for single-component fluids, neither of these equations applies when more than one component exists since the thermodynamic manipulations used in their development no longer hold true, making [1] quite difficult to solve. For simplification purposes, it is often assumed that during the passage of a pressure wave, insufficient time is available for any mass or heat transfer between the two phases. As a result, the fluid quality $\chi$, remains constant, as do $s_G$ and $s_L$ along an isentrope of the bulk fluid. If [1] is expressed as

$$a^2 = -v^2\left(\frac{\partial P}{\partial v}\right)_s \qquad [8]$$

and [7] is substituted into this expression, it follows that

$$a_f^2 = \frac{-v^2}{(1-\chi)\left(\frac{\partial v_L}{\partial P}\right)_s + \chi\left(\frac{\partial v_G}{\partial P}\right)_s} \qquad [9]$$

or, more simply,

$$a_f^2 = \frac{v^2}{(1-\chi)\frac{v_L^2}{a_L^2} + \frac{v_G^2}{a_G^2}}. \quad [10]$$

Since the fluid quality $\chi$, is effectively frozen in [9] and [10], the resultant sound velocity is referred to as the frozen speed of sound, as denoted by the subscript f. To account for different flow regimes, Nguyen *et al.* (1981), in addition to assuming no heat or mass transfer between phases, considered the elastic behavior of the phase boundaries. In doing so, they were able to develop expressions specific to one-dimensional, stratified, slug and homogenous flow.

To obtain the true thermodynamic speed of sound, it was suggested by Groves *et al.* that [1] be solved numerically. As previously mentioned, this approach shall be used here to evaluate $a$ inside the two-phase region of the multicomponent Prudhoe Bay gas. However, since this method is computationally more demanding than that required for $a_f$, it is of value to compare the two solutions, as will also be done.

In actuality, the observed speed of sound is not always that predicted by [1]. With polyatomic fluids, the speed of sound will vary with frequency as a result of the relaxation time required for partitioning of internal energy among the different degrees of molecular freedom (e.g. Richardson 1958; McCormack & Creech 1972; Mistura 1972; Gammon & Douslin 1976). Generally, as the frequency increases, the molecules become stiffer and, subsequently, the observed speed of sound increases. In the case of two-phase fluids, such non-equilibrium effects are accentuated by the added response time required for heat and mass transfer between phases. It has also been suggested that, in two-phase fluids, slippage between phases (Gregor & Rumpf 1975) and surface tension effects (Kieffer 1977) may become significant. However, here, none of these complexities shall be considered, excepting the frozen sound assumption, and their mention is for completeness only.

## 3. COMPUTATIONAL PROCEDURE

### *3.1. Sound velocity*

In its numerical form, [1] may be expressed as

$$a^2 = \left(\frac{\Delta P}{\Delta \rho}\right)_s. \quad [11]$$

To solve this expression for a two-phase multicomponent fluid at a given temperature and pressure, $\Delta P$ was defined as

$$\Delta P = P \times 0.001 \quad [12]$$

and $\Delta\rho$ was defined as

$$\Delta\rho = \rho(T, P) - \rho(T^*, P - \Delta P). \quad [13]$$

The value of $T^*$ was evaluated from the isentropic condition

$$s(T, P) = s(T^*, P - \Delta P). \quad [14]$$

To solve [14] for $T^*$, a modified Newton–Raphson (NR) method (i.e. an NR method with the differential term numerically approximated) was employed. The objective function $\xi$, for this was defined as

$$\xi^{(n)} = s(T, P) - s(T^{*(n)}, P - \Delta P), \quad [15]$$

where superscript $(n)$ denotes the iteration level. To initiate the iterative procedure, the following two estimates of $T^*$ were used:

$$T^{*(0)} = T \quad [16]$$

and

$$T^{*(1)} = T + 1.0\,\text{K}. \quad [17]$$

Convergence was determined by the relation

$$|T^{(n)} - T^{(n-1)}| \leqslant 0.001 \text{ K} \quad [18]$$

and was generally achieved within four iterations.

To determine the value of $\rho$ and $s$ during each iteration, an isobaric–isothermal flash calculation was performed. Details of this are presented further on.

In the single-phase region, sound velocity was calculated using [2] with the specific heat ratio, $\gamma = c_p/c_v$, being evaluated for real fluid behavior and thus treated as a function of both pressure and temperature. In appendix B, expressions are provided for $s$, $c_p$, $c_v$ and $\kappa$, as derived from the PR equation of state. Similar expressions for the SRK equation of the state are presented elsewhere (Picard 1985).

### 3.2. *Flash calculations*

A "flash calculation" is the computational process of determining the equilibrium composition and mole fraction of each phase in a multicomponent multiphase system. It is only flashes at constant $P$ and $T$ which are considered here, and for brevity, these shall be referred to simply as flash calculations.

There are a number of ways in which flash calculations may be performed but regardless of the approach taken, certain fundamental equilibrium and material balance relations must be satisfied. For a two-phase system these are:

*Phase equilibrium*

$$f_{L_i}(T, P, x_j) = f_{G_i}(T, P, y_j), \quad i = 1, n_c; \dagger \quad [19]$$

*Summation of mole fractions*

$$\sum_i x_i = 1, \quad i = 1, n_c, \quad [20]$$

$$\sum_i y_i = 1, \quad i = 1, n_c, \quad [21]$$

$$\sum_i z_i = 1, \quad i = 1, n_c, \quad [22]$$

*Component material balance*

$$y_i G + x_i L = z_i, \quad i = 1, n_c, \quad [23]$$

where [23] may be rewritten as

$$G + L = 1 \quad [24]$$

to give the overall material balance.

In [19]–[24], $f_i$ denotes the fugacity of component $i$ in solution; $x_i$, $y_i$ and $z_i$ are liquid, vapor and composite mole fractions of component $i$, respectively; $G$ and $L$ are the vapor-phase, or gas, and liquid-phase mole fractions, respectively; and $n_c$ is the total number of components in the system. The fugacity, $f_i$, may be obtained from the fugacity coefficient, which is defined as

$$\phi_i = \frac{f_i}{y_i P}. \quad [25]$$

Since $f_i$ is a function of $T$, $P$ and chemical composition, so is $\phi_i$:

$$\phi_i = \phi_i(T, P, y_j) \quad [26]$$

An expression for the fugacity coefficient may be derived using the thermodynamic relation

$$RT \ln(\phi_i) = \int_V^\infty \left[ \left( \frac{\partial P}{\partial n_i} \right)_{T,V,n_j} - \frac{RT}{V} \right] dV - RT \ln(Z), \quad [27]$$

†Phase equilibrium equation [19] is derived from the extremum principle, which defines thermodynamic equilibrium as the condition for which Gibbs free energy is a minimum.

as has been done in appendix B for the PR equation of state. In [27], $V$ is the total system volume, $n_i$ is the number of moles of component $i$ and $Z$ is the compressibility factor, which may be expressed as

$$Z = \frac{P\tilde{v}}{RT}, \quad [28]$$

where $\tilde{v}$ is the molar volume.

In general, the flash calculation problem is one in which $T$, $P$ and $z_i$ are known and the $n_c$-phase equilibrium relations defined by [19], are to be solved for $L$, $G$, $x_i$ and $y_i$ subject to the mole fraction summation and material balance constraints of [20], [21] and [23]. Since these relations form a system of non-linear equations, an iterative procedure is necessary to obtain a solution. The basic procedure which has been used here is as follows.

As is often done, component $k$-factors (i.e. equilibrium ratios $k_i = y_i/x_i$) were chosen as the primary iteration variables, with the mass balance equations being expressed in the following form:

$$\sum_i x_i - \sum_i y_i = \sum_i \frac{z_i(k_i - 1)}{1 + G(k_i - 1)} = 0, \quad i = 1, n_c; \quad [29]$$

$$L = 1 - G; \quad [30]$$

$$y_i = \frac{k_i z_i}{1 + G(k_i - 1)}; \quad [31]$$

and

$$x_i = \frac{y_i}{k_i}. \quad [32]$$

For a given set of $k_i$ and with known values of $z_i$, [29] was solved for $G$ using the NR method. Once $G$ was known, [30] and [31] were used to determine $L$ and $y_i$, respectively. The values of $x_i$ were then determined using [34]. To avoid numerical inconsistencies, the values of $y_i$ and $x_i$ were normalized following their evaluation from [31] and [32], and $G$ was forced to satisfy the condition $0 \leqslant G \leqslant 1.0$.

The phase equilibrium requirements of [19] were considered to have been satisfied and convergence achieved when

$$\epsilon_t = \sum_i \epsilon_i^2 \leqslant 10^{-11}, \quad i = 1, n_c, \quad [33]$$

where $\epsilon_i$ is defined as

$$\epsilon_i = \ln(\phi_{G_i}) - \ln(\phi_{L_i}) + \ln(k_i). \quad [34]$$

Expressions for $\ln(\phi_{G_i})$ and $\ln(\phi_{L_i})$ were determined using [27]. By defining $\epsilon_i$ in terms of [34], it was generally possible to satisfy [33] in the single-phase region. This is not possible if $\epsilon_i$ is expressed in the usual form,

$$\epsilon_i = \ln(f_{G_i}) - \ln(f_{L_i}). \quad [35]$$

If [33] was not satisfied, then values of $k_i$ were improved using a modification of the Mehra *et al.* (1983) correction algorithm. The Mehra *et al.* correction algorithm is given by

$$k_i^{(n+1)} = k_i^{(n)} \left[ \left( \frac{f_{L_i}}{f_{G_i}} \right)^{(n)} \right]^{\delta^{(n)}} \quad [36]$$

$$= k_i^{(n)} [\exp(-\epsilon_i)^{(n)}]^{\delta^{(n)}}, \quad [37]$$

where the bracketed superscript denotes the iteration number and the exponent term $\delta$ is the variable step length, defined by

$$\delta^{(0)} = \delta^{(1)} = 1.0 \quad [38]$$

and

$$\delta^{(n)} = \left| \frac{\epsilon^{(n-1)\mathrm{T}} \cdot \epsilon^{(n-1)}}{\epsilon^{(n-1)\mathrm{T}} \cdot [\epsilon^{(n)} - \epsilon^{(n-1)}]} \right| \delta^{(n-1)} \quad [39]$$

$$= \left| \frac{\epsilon_i^{(n-1)}}{\epsilon^{(n-1)\mathrm{T}} \cdot [\epsilon^{(n)} - \epsilon^{(n-1)}]} \right| \delta^{(n-1)}. \quad [40]$$

The modification in this algorithm results from use of [34], rather than [35], to evaluate $\epsilon_i$. In [39] and [40] the boldface terms are vectors and superscript T is the transpose operator. As was suggested by Mehra *et al.*, acceleration during any one iteration was restricted using [41] so that stability problems arising from poor initial estimates of $k_i$ might be avoided:

$$\max[\Delta \ln(k_i)] = \max[\delta\varepsilon_i] \leqslant 6.0. \quad [41]$$

Selection of the Mehra *et al.* correction algorithm was made on the basis of its good acceleration properties and because, compared to the more familiar quasi-Newton methods, it required storage of only one vector per iteration rather than an entire inverse Jacobian matrix.

In applying flash calculations to the iterative solution of [15], it was appropriate, for computational efficiency, to use $k$-factors from the previous flash as starting values for the current one. Initial $k$-factors for the very first flash or single flash calculations were obtained using the expression presented by Wilson (1969):

$$k_i = \frac{\exp\left[5.37(1+\omega_i)\left(1 - \frac{T_{c_i}}{T}\right)\right] P_{c_i}}{P}, \quad [42]$$

where $\omega$ is the Pitzer acentric factor and subscript c denotes critical property.

In order to evaluate $\ln(\phi_{\mathrm{L}_i})$ and $\ln(\phi_{\mathrm{G}_i})$, the compressibility factors $Z_{\mathrm{L}}$ and $Z_{\mathrm{G}}$ first had to be determined, as is apparent from [27]. This was done by writing the equation of state for each phase in terms of its compressibility factor, resulting in two expressions of the form

$$F(Z) = Z^3 + bZ^2 + cZ + d = 0. \quad [43]$$

These were then solved separately for $Z_{\mathrm{L}}$ and $Z_{\mathrm{G}}$. In [43] the coefficients $b$, $c$ and $d$ are functions of $R$, $T$, $P$, $\hat{a}$ and $\hat{b}$ (see appendix B for the PR equation of state). Since [43] is a cubic equation with real coefficients it will have three possible solutions with at least one always being real. The normal procedure for selecting a compressibility factor from these solutions is, if only one real root occurs, then that is the compressibility factor, otherwise, for liquid-phase calculations the smallest root is chosen and for vapor-phase calculations the largest root is chosen. When $k$-factor estimates are poor, or the flash temperature and pressure are close to that of the true critical point, this procedure can result in a trivial solution. That is, a single phase may be predicted when in fact two phases exist. To help avoid this problem, the Gundersen (1982) algorithm was employed. However, the roots of [43] were solved analytically (Perry & Chilton 1973), rather than numerically as Gundersen had.

Once the flash calculations had been performed it was necessary to evaluate thermodynamic properties of the bulk fluid. The following equations were useful in performing this task:

(1) molecular weight $M$,

$$M = \sum_i z_i \cdot amw_i, \quad i = 1, n_c, \quad [44]$$

where $amw_i$ is the molecular weight of component $i$;

(2) quality, $\chi$

$$\chi = \frac{g\, M_{\mathrm{G}}}{M}. \quad [45]$$

## 4. RESULTS AND DISCUSSION

### 4.1. Evaluation of the PR and SRK equations of state

Both the PR and SRK equations of state are noted for their ability to provide quite accurate vapor densities and generate reliable equilibrium ratios. However, neither is able to provide liquid densities with the same level of acceptability, although the PR equation of state is somewhat better than the SRK. To establish further weaknesses or strengths of these equations, a good test is their ability to accurately calculate the thermodynamic speed of sound.

In figures 1–3, the thermodynamic sound velocities calculated from the PR and SRK equations of state are compared with experimental data for methane (Stray 1974), ethane (Tsumura & Stray 1977) and propane (Noury *et al.* 1958), respectively. The symbols $P_r$ and $T_r$ used in these figures denote reduced pressure and reduced temperature, respectively. To indicate the degree of non-ideality at the conditions considered, the thermodynamic speed of sound, $a$, has been reduced by $a^\circ$, the ideal gas speed of sound (Note: $a^\circ$ is independent of pressure). The values for $a^\circ$ are presented in table 1.

The sudden drop in sound velocity which occurs along certain isotherms in each of figures 1–3 (e.g. $T_r = 0.966$ in figure 1), indicates a change in fluid behavior. To the right of this dip, the fluid behaves as a liquid (i.e. along a given isotherm an increase in pressure results in an increase in $a$); and to the left, as a vapor (i.e. along a given isotherm an increase in pressure results in a decrease in $a$). Although neither equation of state can be expected to provide extremely accurate predictions

Table 1. Ideal gas sound velocities

| Methane | | Ethane | | Propane | |
|---|---|---|---|---|---|
| $T_r$ | $a^\circ$ (m/s) | $T_r$ | $a^\circ$ (m/s) | $T_r$ | $a^\circ$ (m/s) |
| 0.525 | 262.15 | 0.327 | 190.08 | 0.941 | 270.04 |
| 0.787 | 322.10 | 0.458 | 222.79 | 0.982 | 275.29 |
| 0.966 | 356.60 | 0.589 | 250.00 | 1.009 | 278.73 |
| 1.260 | 405.47 | 0.720 | 273.56 | 1.077 | 287.15 |
| 1.574 | 449.62 | 0.851 | 294.56 | | |
| | | 0.982 | 313.71 | | |
| | | 1.058 | 324.13 | | |

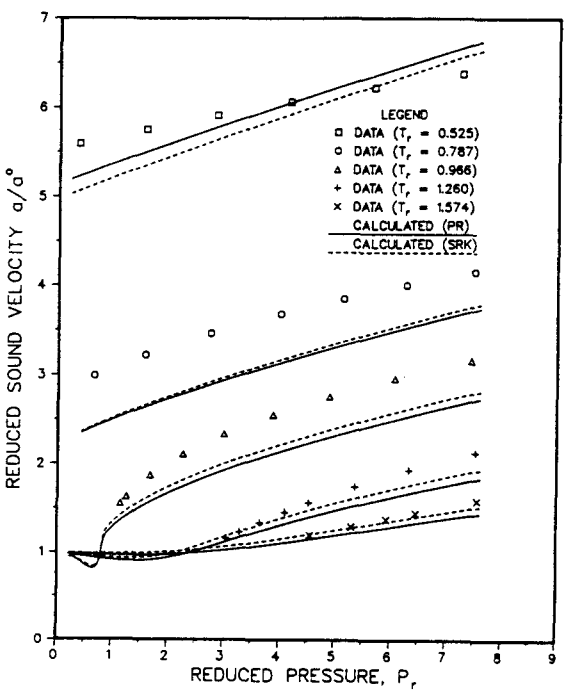


Figure 1. Thermodynamic speed of sound in methane.

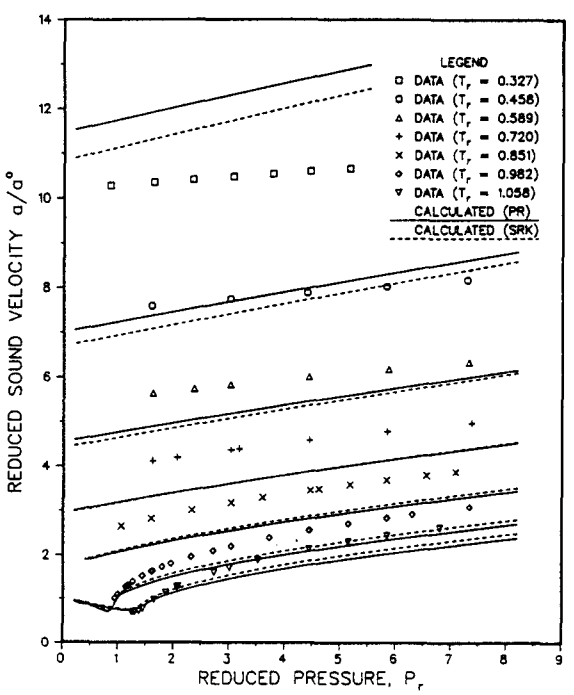


Figure 2. Thermodynamic speed of sound in ethane.

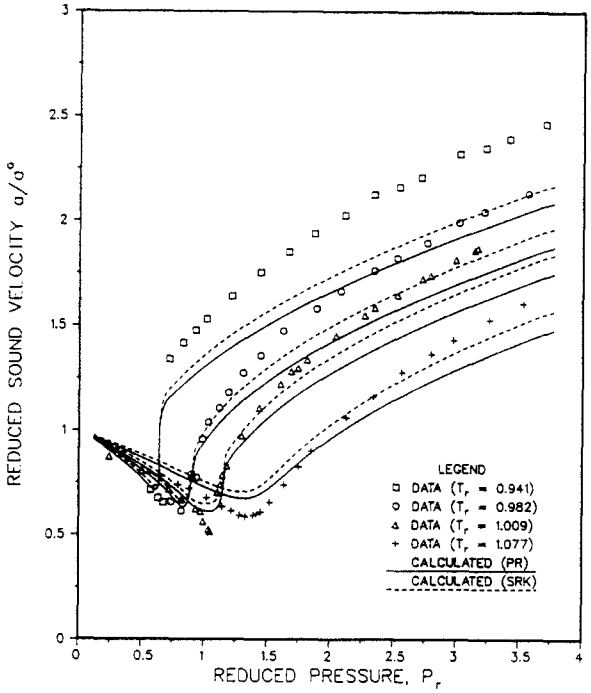


Figure 3. Thermodynamic speed of sound in propane.

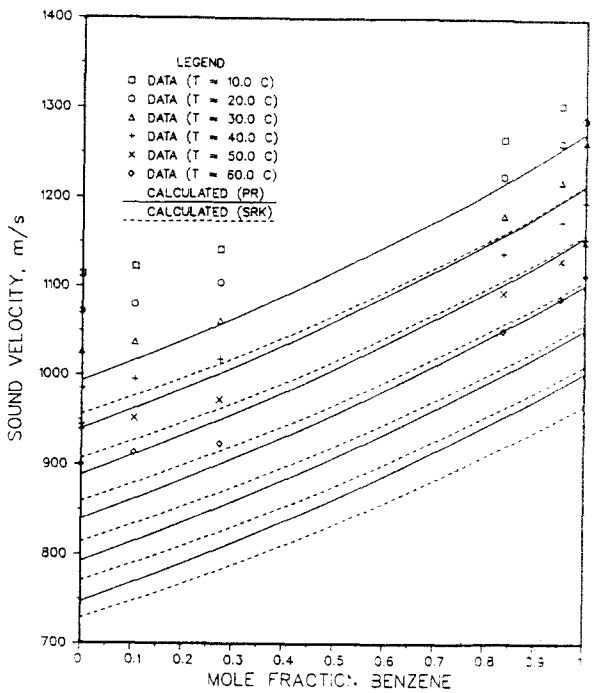


Figure 4. Thermodynamic speed of sound in benzene–hexane mixtures.

of $a$, it is important to note that each equation obeyed the basic trends observed in the data. In the liquid region it can be seen that neither equation of state is able to accurately predict $a$ (i.e. errors as high as, approx. 25, 35 and 20% occurred in figures 1–3, respectively), as might have been expected. Based on the limited vapor data in figures 2 and 3, application of these equations to vapors would appear to be much more reasonable (i.e. errors of $< 10\%$).

To evaluate the mixing rules used for both equations of state, sound velocity calculations have been made for the binary benzene–hexane liquid-phase data of Snyder & Snyder (1974), as shown in figure 4. Although graphically the comparison between theory and experiment appears to be quite poor, the predictions are, at most, only 10% in error. This is surprisingly good considering the data are for a completely liquid system. The important thing to note here, is that errors do not increase upon mixing. This would indicate that the mixing rules are quite acceptable and, thus, give credibility to values of $a$ calculated for multicomponent fluids.

### *4.2. Sound velocity in two-phase multicomponent fluids*

Since neither equation of state performed significantly better than the other, in terms of sound velocity predictions, selection of one for the calculation of $a$ and $a_f$ in two-phase multicomponent fluids becomes a somewhat arbitrary decision. Here, the PR equation of state was chosen.

In figure 5, the thermodynamic speed of sound, $a$, has been calculated along various isobars of the multicomponent Prudhoe Bay gas described by Groves *et al.* For each of the isobars shown, the fluid appears on the right of figure 5 as a completely gaseous mixture. Moving towards the left, a sudden drop in sound velocity appears for isobars 1–7 MPa, indicating the onset of condensation—as can be confirmed by referring to the phase envelope presented in figure 6. The occurrence of such behavior has been confirmed by the decompression data obtained by Groves (1976) for Prudhoe Bay gas. In these data, a sudden reduction in expansion wave velocity was observed at approximately the calculated dew point. The reason for this sudden drop in $a$, is the fact that the formation of a second phase, compressibility of the fluid decreases. The effects of this are more significant at the higher pressures. Moving further to the left, a sudden jump in sound velocity appears as isobars 2–7 MPa leave the two-phase region. Here, however, the greatest effects occur at the lower pressures. To the left of the sudden jump, the fluid behaves as a liquid and hence the sound velocity increases as the temperature decreases. Since the 1 MPa isobar remains in the

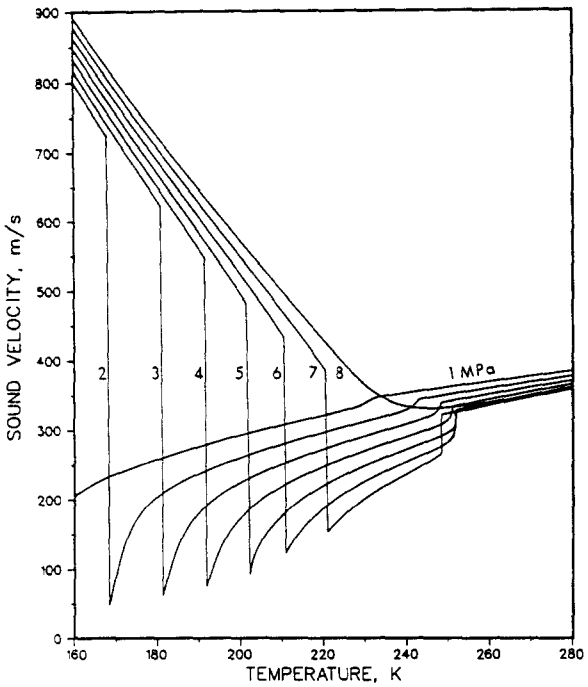


Figure 5. Thermodynamic speed of sound in Prudhoe Bay mixture.

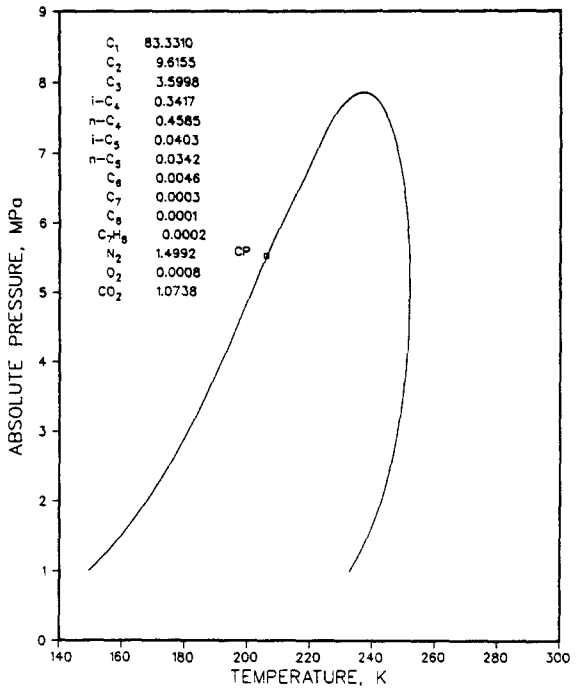


Figure 6. Vapor–liquid equilibrium diagram of Prudhoe Bay mixture.

two-phase region, for the temperature range of the figure, this sudden jump is not shown. Moving from right to left along the 8 MPa isobar, which never intersects the two-phase region, it can be seen that, initially, the single-phase fluid behaves as a gas (i.e. sound velocity decreases with a decrease in temperature) and at approx. 240 K, begins to behave as a liquid (i.e. sound velocity increases with a decrease in temperature). As a philosophical point, it is of interest to note that the 6 and 7 MPa isobars pass through the retrograde region (see figure 6) and, therefore, are in the vapor phase prior to entering the two-phase region and also after leaving, yet upon leaving the two-phase region, the fluid behaves, in terms of sound velocity, as a liquid.

If sound velocity in the two-phase region is calculated using [10] for the frozen speed of sound, then the results are those shown in figure 7. In comparison with the thermodynamic values of figure 5 it can be seen that the frozen assumption does not produce a sudden drop in sound velocity upon entering the two-phase region and, subsequently, predicts higher sound velocities in this region.

It should be mentioned that in developing figure 5, some computational difficulties were encountered along the 5 MPa isobar between the temperatures of 201 and 210 K. That is, calculations converged on a single-phase solution when, based on figure 6, two phases must exist. The curve was therefore completed by extrapolation. The reason that only the 5 MPa isobar was affected and not the others is that it passes through the difficult region of the critical point, as can be seen from figure 6. In generating the 5 MPa curve for figure 7, such difficulties were not encountered, thus, indicating that the problem was in part, a result of the numerical procedure used in calculating $a$.

## 5. CONCLUSIONS

(1) Both the PR and SRK equations of state are weak in predicting sound velocities in liquids, however, each shows some promise for application to vapors (i.e. < 10% error).
(2) Both equations of state are able to predict the basic trends observed in the available experimental data.
(3) Mixing rules for the equations of state appear to be quite acceptable, thus giving credibility to sound velocity calculations for multicomponent mixtures.
(4) To more fully examine the usefulness of the PR and SRK, or any other equations of state, in predicting sound velocities, additional experimental data are required.

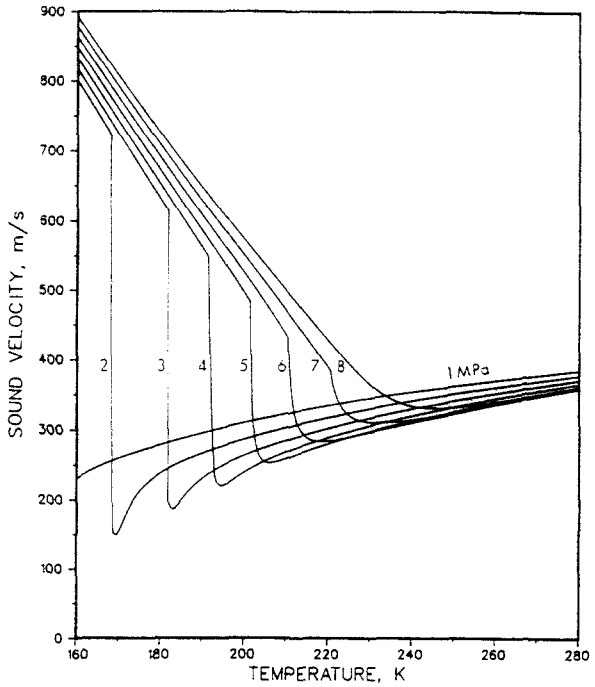


Figure 7. Frozen speed of sound in Prudhoe Bay mixture.

(5) Although the assumption of no heat or mass transfer between phases greatly simplifies the calculation of sound velocity in two-phase multicomponent fluids, it predicts somewhat higher speeds than the truly thermodynamic solution and is not able to predict the sudden drop in sound velocity upon intersection of the dew line.
(6) The attenuation of sound velocity inside the two-phase region of multicomponent fluids is an interesting phenomenon which is worthy of further study.

*Acknowledgement*—The financial support provided by the University of Calgary is greatly appreciated.

## REFERENCES

API 1977 *Technical Data Book*: *Petroleum Refining*, Vol. II. API.

GAMMON, B. E. & DOUSLIN, D. R. 1976 The velocity of sound and heat capacity in methane from near-critical to subcritical conditions and equation-of-state implications. *J. chem. Phys.* **64,** 203–218.

GREGOR, W. & RUMPF, H. 1975 Velocity of sound in two-phase media. *Int. J. Multiphase Flow* **1,** 753–769.

GROVES, T. K. 1976 Measured velocity of decompression waves in natural gases in pipe lines. Report prepared for Foothills Pipe Lines (Yukon) Ltd.

GROVES, T. K., BISHNOI, P. R. & WALLBRIDGE, J. M. E. 1978 Decompression wave velocities in natural gases in pipe lines. *Can. J. chem. Engng* **56,** 664–668.

GUNDERSEN, T. 1982 Numerical aspects of the implementation of cubic equations of state in flash calculation routines. *Comput. chem. Engng* **6,** 245–255.

KIEFFER, S. W. 1977 Sound speed in liquid–gas mixtures: water–steam. *J. geophys. Res.* **82,** 2895–2904.

MCCORMACK, F. J. & CREECH, H. W. 1972 17-Moment theory of sound propagation in polyatomic gases. *J. acoust. Soc. Am.* **51,** 900–909.

MEHRA, R. K., HEIDEMANN, R. A. & AZIZ, K. 1983 An accelerated successive substitution algorithm. *Can. J. chem. Engng* **61,** 590–596.

MICHAELIDES, E. E. & ZISSIS, K. L. 1983 Velocity of sound in two-phase mixtures. *Int. J. Heat Fluid Flow* **4,** 79–84.

MISTURA, L. 1972 Sound propagation near a critical point in multicomponent fluid systems. *J. chem. Phys.* **57**, 2311–2317.

NGUYEN, D. L., WINTER, E. R. F. & GREINER, M. 1981 Sonic velocity in two-phase systems. *Int. J. Multiphase Flow* **7**, 311–320.

NOURY, J., LACAM, A., M'HIRSI, A., BERGEON, R., GALATRY, L. & VODOR, B. 1958 Measurement of ultrasonic velocity in compressed fluids and determination of some thermodynamic properties. In *Joint Conf. on Thermodynamic and Transport Properties of Fluids*, pp. 48–56. Inst. Mech. Engrs, London.

OELLRICH, L., PLÖCKER, U., PRAUSNITZ, J. M. & KNAPP, H. 1981 Equations of state methods for computing phase equilibria and enthalpies. *Int. chem. Engng* **21**, 1–16.

PENG, D. & ROBINSON, D. B. 1976 A new two-constant equation of state. *Ind. Engng Chem. Fundam.* **15**, 59–64.

PERRY, R. H. & CHILTON, C. H. 1973 *Chemical Engineer's Handbook*, 5th edn. McGraw-Hill, New York.

PICARD, D. J. 1985 A non-isentropic model for simulating decompression characteristics of high pressurre multicomponent pipeline gases. M.Eng. Thesis, Univ. of Calgary, Calgary, Alberta.

REID, R. C., PRAUSNITZ, J. M. & SHERWOOD, T. K. 1977 *The Properties of Gases and Liquids*, 3rd edn. McGraw-Hill, New York.

RICHARDSON, E. G. 1958 Derivation of some thermodynamic parameters of fluids from measurements of ultrasonic propagation therein. In *Joint Conf. on Thermodynamic and Transport Properties of Fluids*, pp. 34–36. Inst. Mech. Engrs, London.

SNYDER, W. J. & SNYDER, J. R. 1974 Velocity of sound in binary mixtures of benzene, hexane, and methanol at 0–65°C. *J. chem. Engng Data* **19**, 270–274.

SOAVE, G. 1972 Equilibrium constants from a modified Redlich–Kwong equation of state. *Chem. Engng Sci.* **27**, 1197–1203.

STRAY, G. C. 1974 Velocity of sound in dense fluid methane. *Cryogenics* **14**, 367–370.

TSUMURA, R. & STRAY, G. C. 1977 Speed of sound in saturated and compressed fluid ethane. *Cryogenics* **17**, 195–200.

WILSON, G. 1969 A modified Redlich–Kwong equation of state, application to general physical data calculations. Presented at the *AIChE 65th natn. Mtg*, Cleveland, Ohio, Paper No. 15C.

## APPENDIX A

*PR equation of state*

$$P = \frac{RT}{\tilde{v} - \hat{b}} - \frac{\hat{a}(T)}{\tilde{v}(\tilde{v} + \hat{b}) + \hat{b}(\tilde{v} - \hat{b})}, \quad [A.1]$$

$$\hat{b} = 0.07780 \frac{RT_c}{P_c}, \quad [A.2]$$

$$\hat{a}(T) = \hat{a}(T_c)\,\hat{\alpha}(T_r, \omega), \quad [A.3]$$

$$\hat{a}(T_c) = 0.45724 \frac{R^2 T_c^2}{P_c}, \quad [A.4]$$

$$\hat{\alpha}(T_r, \omega) = [1 + \hat{m}(1 - T_r^{0.5})]^2, \quad [A.5]$$

$$\hat{m} = 0.377464 + 1.54226\omega - 0.26992\omega^2. \quad [A.6]$$

*SRK equation of state*

$$P = \frac{RT}{\tilde{v} - \hat{b}} - \frac{\hat{a}(T)}{\tilde{v}(\tilde{v} + \hat{b})}, \quad [A.7]$$

$$\hat{b} = 0.08664 \frac{RT_c}{P_c}, \quad [A.8]$$

$$\hat{a}(T) = \hat{a}(T_c)\,\hat{\alpha}(T_r, \omega), \tag{A.9}$$

$$\hat{a}(T_c) = 0.42747\frac{R^2T_c^2}{P_c}, \tag{A.10}$$

$$\hat{\alpha}(T_r, \omega) = [1 + \hat{m}(1 - T_r^{0.5})]^2, \tag{A.11}$$

$$\hat{m} = 0.480 + 1.574\omega - 0.176\omega^2. \tag{A.12}$$

*Mixing rules*

$$\hat{b} = \sum_i y_i \hat{b}_i, \quad i = 1, n_c, \tag{A.13}$$

$$\hat{a} = \sum_i \sum_j y_i y_j \hat{a}_{ij}, \quad i, j = 1, n_c, \tag{A.14}$$

$$\hat{a}_{ij} = (1 - \hat{\delta}_{ij})\,\hat{a}_i^{0.5}\,\hat{a}_j^{05}. \tag{A.15}$$

In [A.1]–[A.15], $\hat{\delta}$ is the binary interaction coefficient, $y$ denotes mole fraction, superscript $\hat{}$ indicates equation of state parameter, superscript $\tilde{}$ denotes molar specific property, subscript r denotes reduced property and subscripts $i$ and $j$ indicate chemical component.

Values used for the binary interaction coefficient were those presented by Oellrich *et al.* (1981). All critical constants and acentric factors were obtained from Reid *et al.* (1977).

## APPENDIX B

*Thermodynamic Properties—PR Equation of State*

*(1) Internal energy, $\tilde{u}$*

$$\tilde{u} - \tilde{u}^\circ = -\int_{\tilde{v}}^{\infty}\left[T\left(\frac{\partial \hat{P}}{\partial T}\right)_{\tilde{v}} - P\right]d\tilde{v} \tag{B.1}$$

aside,

$$\left(\frac{\partial \hat{P}}{\partial T}\right)_{\tilde{v}} = \frac{R}{\tilde{v} - \hat{b}} - \frac{\hat{a}'}{\tilde{v}(\tilde{v} + \hat{b}) + \hat{b}(\tilde{v} - \hat{b})} \tag{B.2}$$

$$= \frac{P}{T} + \frac{\dfrac{(\hat{a} - \hat{a}'T)}{T}}{\tilde{v}(\tilde{v} + \hat{b}) + \hat{b}(\tilde{v} - \hat{b})} \tag{B.3}$$

(note: $\hat{a}'$ equals $d\hat{a}/dT$) therefore,

$$\tilde{u} - \tilde{u}^\circ = (\hat{a} - \hat{a}'T)\int_{\infty}^{\tilde{v}} \frac{d\tilde{v}}{\tilde{v}(\tilde{v} + \hat{b}) + \hat{b}(\tilde{v} - \hat{b})} \tag{B.4}$$

$$= \frac{\hat{a} - \hat{a}'T}{2.828\hat{b}} \ln\left(\frac{\tilde{v} - 0.414\hat{b}}{\tilde{v} + 2.414\hat{b}}\right), \tag{B.5}$$

$$\tilde{u}^\circ = \sum_i y_i \tilde{u}_i^\circ, \quad i = i, n_c. \tag{B.6}$$

*(2) Enthalpy, $\tilde{h}$*

$$\tilde{h} - \tilde{h}^\circ = P\tilde{v} - RT - \int_{\tilde{v}}^{\infty}\left[T\left(\frac{\partial \hat{P}}{\partial T}\right)_{\tilde{v}} - P\right]d\tilde{v} \tag{B.7}$$

$$= \frac{\hat{a} - \hat{a}'T}{2.828\hat{b}} \ln\left(\frac{\tilde{v} - 0.414\hat{b}}{\tilde{v} + 2.414\hat{b}}\right) + P\tilde{v} - RT, \tag{B.8}$$

$$\tilde{h}^\circ = \sum_i y_i \tilde{h}_i^\circ, \quad i = 1, n_c. \tag{B.9}$$

*(3) Entropy, $\tilde{s}$*

$$\tilde{s} - \tilde{s}^\circ = -R\ln(P) + R\ln(Z) - \int_{\tilde{v}}^{\infty}\left[\left(\frac{\partial P}{\partial T}\right)_{\tilde{v}} - \frac{R}{\tilde{v}}\right]d\tilde{v} \quad [B.10]$$

$$= R\ln\left(\frac{\tilde{v}-\hat{b}}{RT}\right) - \frac{\hat{a}'}{2.828\hat{b}}\ln\left(\frac{\tilde{v}-0.414\hat{b}}{\tilde{v}+2.414\hat{b}}\right), \quad [B.11]$$

$$\tilde{s}^\circ = \sum_i y_i \tilde{s}_i^\circ - R\sum_i y_i \ln(y_i), \quad i = 1, n_c. \quad [B.12]$$

*(4) Heat capacity at constant volume $\tilde{c}_v$*

$$\tilde{c}_v - \tilde{c}_v^\circ = -T\int_{\tilde{v}}^{\infty}\left(\frac{\partial^2 P}{\partial T^2}\right)_{\tilde{v}} d\tilde{v} \quad [B.13]$$

$$= \left(\frac{\partial(\tilde{u}-\tilde{u}^\circ)}{\partial T}\right)_{\tilde{v}} \quad [B.14]$$

$$= \frac{-\hat{a}''T}{2.828\hat{b}}\ln\left(\frac{\tilde{v}-0.414\hat{b}}{\tilde{v}+2.414\hat{b}}\right), \quad [B.15]$$

$$\tilde{c}_v^\circ = \sum_i y_i \tilde{c}_{v_i}^\circ = \sum_i y_i(\tilde{c}_{p_i}^\circ - R), \quad i = 1, n_c. \quad [B.16]$$

*(5) Heat capacity at constant pressure, $\tilde{c}_p$*

$$\tilde{c}_p - \tilde{c}_p^\circ = -R - \frac{T\left(\frac{\partial P}{\partial T}\right)_{\tilde{v}}^2}{\left(\frac{\partial P}{\partial \tilde{v}}\right)_T} - T\int_{\tilde{v}}^{\infty}\left(\frac{\partial^2 P}{\partial T^2}\right)_{\tilde{v}} d\tilde{v} \quad [B.17]$$

$$= \left(\frac{\partial(\tilde{h}-\tilde{h}^\circ)}{\partial T}\right)_p \quad [B.18]$$

$$= -R - \frac{T[R\tilde{v}(\tilde{v}+\hat{b}) + (R\hat{b}-\hat{a}')(\tilde{v}-\hat{b})]^2}{2\hat{a}(\tilde{v}+\hat{b})(\tilde{v}-\hat{b})^2 - RT[\tilde{v}(\tilde{v}+\hat{b}) + \hat{b}(\tilde{v}-\hat{b})]^2}$$

$$\times \frac{-\hat{a}''T}{2.828\hat{b}}\ln\left(\frac{\tilde{v}-0.414\hat{b}}{\tilde{v}+2.414\hat{b}}\right), \quad [B.19]$$

$$\tilde{c}_p^\circ = \sum_i y_i \tilde{c}_{p_i}^\circ, \quad i = 1, n_c. \quad [B.20]$$

*(6) Specific heat ratio, $\gamma$*

$$\gamma = \frac{\tilde{c}_p}{\tilde{c}_v} \quad [B.21]$$

*(7) Isothermal coefficient of volumetric expansion, $\kappa$*

$$\kappa = -\frac{1}{\tilde{v}}\left(\frac{\partial \tilde{v}}{\partial P}\right)_T \quad [B.22]$$

aside,

$$\left(\frac{\partial P}{\partial \tilde{v}}\right)_T = \frac{-RT}{(\tilde{v}-\hat{b})^2} + \frac{2\hat{a}(\tilde{v}+\hat{b})}{[\tilde{v}(\tilde{v}+\hat{b}) + \hat{b}(\tilde{v}-\hat{b})]^2} \quad [B.23]$$

$$= \frac{-RT[\tilde{v}(\tilde{v}+\hat{b}) + \hat{b}(\tilde{v}-\hat{b})]^2 + 2\hat{a}(\tilde{v}+\hat{b})(\tilde{v}-\hat{b})^2}{[\tilde{v}(\tilde{v}+\hat{b})(\tilde{v}-\hat{b}) + \hat{b}(\tilde{v}-\hat{b})^2]^2} \quad [B.24]$$

therefore,

$$\kappa = \frac{-[\tilde{v}(\tilde{v}+\hat{b})(\tilde{v}-\hat{b})+\hat{b}(\tilde{v}-\hat{b})^2]^2}{2\hat{a}\tilde{v}(\tilde{v}+\hat{b})(\tilde{v}-\hat{b})^2 - RT\tilde{v}[\tilde{v}(\tilde{v}+\hat{b})+\hat{b}(\tilde{v}-\hat{b})]^2}. \quad [B.25]$$

*(8) $\hat{a}'$*

$$\hat{a}' = \frac{d\hat{a}}{dt} = \sum_i \sum_j y_i y_j \hat{a}'_{ij}, \quad i,j = 1, n_c, \quad [B.26]$$

aside,

$$\hat{a}'_{ij} = \frac{1-\hat{\delta}_{ij}}{2}\left[\left(\frac{\hat{a}_j}{\hat{a}_i}\right)^{0.5} a'_i + \left(\frac{\hat{a}_i}{\hat{a}_j}\right)^{0.5} a'_j\right], \quad [B.27]$$

$$a'_i = \hat{a}(T_{c_i})\,\hat{\alpha}'_i \quad [B.28]$$

and

$$\hat{\alpha}'_i = -\frac{\hat{m}_i}{T}(\hat{\alpha}_i T_{r_i})^{0.5} = \frac{\hat{m}_i T_{r_i}^{0.5}}{T\hat{\alpha}_i^{0.5}}\hat{\alpha}_i \quad [B.29]$$

therefore,

$$\hat{a}'_{ij} = \frac{\hat{a}_{ij}}{2T}(\hat{\theta}_i + \hat{\theta}_j) \quad [B.30]$$

where

$$\hat{\theta}_i = -\hat{m}_i\left(\frac{T_{r_i}}{\alpha_i}\right)^{0.5}. \quad [B.31]$$

*(9) $\hat{a}''$*

$$\hat{a}'' = \frac{d^2\hat{a}}{dT^2} = \sum_i \sum_j y_i y_j \hat{a}''_{ij}, \quad i,j = 1, n_c, \quad [B.32]$$

$$\hat{a}''_{ij} = \frac{\hat{a}_{ij}}{4T^2}[2\hat{\theta}_i\hat{\theta}_j - (\hat{\theta}_i + \hat{\theta}_j)]. \quad [B.33]$$

*(10) Fugacity coefficient, $\phi_i$*

$$\ln(\phi_i) = \frac{1}{RT}\int_V^\infty \left[\left(\frac{\partial P}{\partial n_i}\right)_{T,V,n_j} - \frac{RT}{V}\right]dV - RT\ln(Z) \quad (i \neq j) \quad [B.34]$$

$$= \frac{\hat{b}_i}{\hat{b}}(Z-1) - \ln(Z-B) - \frac{A}{2.828B}\cdot\left(\frac{2\sum_i y_i \hat{a}_{ij}}{\hat{a}} - \frac{\hat{b}_i}{\hat{b}}\right)\ln\left(\frac{Z+2.414B}{Z-0.414B}\right). \quad [B.35]$$

where

$$A = \frac{\hat{a}P}{R^2T^2} \quad [B.36]$$

and

$$B = \frac{\hat{b}P}{RT}. \quad [B.37]$$

*(11) Compressibility equation, $F(Z)$*

$$F(Z) = Z^3 - (1-B)Z^2 + (A - 3B^2 - 2B)Z - (AB - B^2 - B^3) = 0. \quad [B.38]$$

Correlations for the ideal gas properties, $h^\circ$, $c_p^\circ$ and $s^\circ$, were obtained from the *API Technical Data Book: Petroleum Refining* (1977).